Received: 22 December 2018 | Revised: 28 January 2020 | Accepted: 4 February 2020

DOI: 10.1002/joc.6518

RESEARCH ARTICLE

International Journal of Climatology RMetS

Comparison between observations and gridded data sets over complex terrain in the Chilean Andes: Precipitation and temperature

Vanúcia Schumacher[1] | **Flávio Justino**[1] | **Alfonso Fernández**[2] | **Oliver Meseguer-Ruiz**[3] | **Pablo Sarricolea**[4] | **Alcimoni Comin**[1] | **Luan Peroni Venancio**[1] | **Daniel Althoff**[1]

[1]Department of Agriculture Engineering, Universidade Federal de Viçosa, Viçosa, Brazil

[2]Department of Geography and Mountain GeoScience Group, Universidad de Concepción, Concepción, Chile

[3]Departamento de Ciencias Históricas y Geográficas, Universidad de Tarapacá, Arica, Chile

[4]Department of Geography, Universidad de Chile, Santiago, Chile

Correspondence
Vanúcia Schumacher, Department of Agricultural Engineering, Universidade Federal de Viçosa, Viçosa, Brazil.
Email: vanucia-schumacher@hotmail.com

Funding information
Coordination for the Improvement of Higher Education Personnel (CAPES); CNPq, Grant/Award Number: 306181-20169; FAPEMIG, Grant/Award Number: PPM00773-18; FONDECYT, Grant/Award Numbers: 11160059, 11160454, 1171065

Abstract

This study describes the performance of five gridded data sets in reproducing precipitation and/or temperature over the complex terrain in the high Chilean Andes. The relationship of instrumental observations and the gridded data sets with climate modes of variability and the trends of indices of climate extremes are also explored between the period 1980–2015. The mismatches between gridded data sets are larger in northern and southern regions in relation to precipitation, while for temperature, disagreement is higher in central region. However, better results are delivered by the Climatic Research Unit and Global Precipitation Climatology Centre followed by Re-Analysis Interim Project. The El Niño Southern Oscillation and Pacific Decadal Oscillation indices are well correlated with precipitation in North and South Chile. Additional, trend analyses reveal a significant downward (upward) tendency for precipitation (temperature), especially in central region, delivered by observed and the majority of gridded data sets. Furthermore, the consecutive number of dry days is increasing in all regions at the annual scale. This study allows a better understanding of the capacity of global data sets and thus contributes to further climate research within this Andean region.

KEYWORDS

climate indices, gridded data sets, precipitation and temperature trends, reanalyses

1 | INTRODUCTION

Due to its complex topography and latitudinal extent, Chile exhibits different climatic zones, from tropical to extratropical featuring desertic, volcanic, lacustrine and icy landscapes that define extreme gradients, including the arid north in Atacama and the extreme precipitation in Southern Patagonia (Garreaud, 2009; Sarricolea *et al.*, 2017). Central Chile concentrates the country's population, including the densely populated Metropolitan Santiago region, as well as important sectors of the economic activity. In this region, millions depend on steady water availability to support hydropower generation, and activities associated with agriculture, industry and tourism, especially during the dry season (Masiokas *et al.*, 2012). As water availability depends on the local climate variability, changes in temperature and precipitation may affect future water resources and availability in

several regions in Chile (Bradley, 2006; Sarricolea and Romero, 2015; Boisier *et al*., 2016).

As a number of studies indicate that the behavior of glaciers and river flows in high Andes are sensitive to warming trends and precipitation changes under ongoing climate change (Vuille *et al*., 2008; Urrutia and Vuille, 2009; Rabatel *et al*., 2013; Neukom *et al*., 2015; Ragettli *et al*., 2016), it becomes evident that the characterization of these meteorological variables is crucial to understand how climate change may impact these regions. On the other hand, despite recent encouraging initiatives (Alvarez-Garreton *et al*., 2018), obtaining continuous and accurate weather information in the Andean mountain range is still a difficult task (Manz *et al*., 2016). The Andean complex orography makes it difficult to maintain and expand the network of meteorological stations and the development of reliable measurements of the spatial and long-term historical observations (Cowtan and Way, 2014).

In this context, gridded data sets are useful tools to overcome the dearth of observations, allowing the development of long-term climate analyses and monitoring (e.g., Gu and Adler, 2019). Among several applications, gridded data sets are utilized for data assimilation, comparison with observations, forcing data for global and regional models, and to investigate atmospheric process and climatic variability during recent decades (Lorenz and Kunstmann, 2012; Cortés *et al*., 2016; Huang *et al*., 2016; Zazulie *et al*., 2017; Serrano-Notivoli *et al*., 2018). Reanalyses products also have been widely used for statistical, dynamical and hydrologic downscaling (Soares *et al*., 2012; Bieniek *et al*., 2016; El-Samra *et al*., 2017). These downscaled climate fields can be used as input in other climate models, especially in complex terrain of the Andes, helping to understand the physical and dynamic processes in regions of irregular topography (Fernández and Mark, 2016; Comin *et al*., 2018).

However, the performance of these applications depends on the accuracy and ability of the gridded data sets to reproduce local climatic features. Indeed, gridded data sets have shown great performance on the global scale, but the improvements needed for these data sets to be accurate at the regional scale are important due to large uncertainties (e.g., Angélil *et al*., 2016). This is more critical in mountain areas, where complex terrain induces large biases and gradients of precipitation and near surface temperature (Silva *et al*., 2011; Schauwecker *et al*., 2014, 2017).

Some studies have evaluated temperature and precipitation changes in the Southern Hemisphere at the regional scale and using different gridded products (e.g., Bromwich *et al*., 2011). Although gridded data sets have been subjected to diverse evaluations worldwide (Morice *et al*., 2012; Rapaić *et al*., 2015), there is a lack of studies focusing on the complex Chilean terrain. Nearby areas have been studied, however, such as the case of a comparison of precipitation depicted by CFSR and MERRA reanalyses and combined products over basins in Bolivia, show overestimation of precipitation over the Altiplano basin (Blacutt *et al*., 2015).

This study aims to presents the results of the performance of five widely used global gridded data sets in reproducing precipitation and surface temperature along the Chilean Andes between (~17°–40°S for the period 1980–2015). This study also includes an analysis of climate indices associated with precipitation using the observational and gridded data sets, as well as the relationship of the gridded products with climate modes of variability that are known to be important in this region. Section 2 describes the data and methods utilized. Section 3 presents results of the performance of the gridded data sets: (a) mean annual, (b) seasonal value and (c) spatio-temporal trends of precipitation and near surface temperature relative to instrumental observations. Finally, in Section 4, we draw conclusions of our findings.

2 | DATA AND METHODS

2.1 | Station observations

Station observation of precipitation and surface temperature were used to evaluate gridded data sets. These measurements are maintained by the Chilen Water Directorate (Dirección General de Aguas) and the Chilean Weather Directorate (Dirección Meteorológica de Chile) and are available through the Climate Explorer of the Center for Climate and Resilence (http://explorador.cr2.cl). In this study, high Chilean Andes climatology with complex topography is represented by all weather stations above 500 m a.s.l. To achieve the most representative and consistent data for verification, we selected only daily data with less than 10% of missing days in each monthly series for the period. Individual records were considered outliers and discarded when monthly totals exceeded four times the *SD* above the mean. No interpolation method was attempted to fill gaps. Beyond these considerations, we believe that these data sets are a good representation of Chilean observations without interference by interpolation and data filling.

Given that the distribution of data in Andes is very sparse for a long-term climatic assessment, measurements were selected considering two periods from 1980 to 2015 and from 1990 to 2015, since little stations span between 1980 and 2015 intervals. The observations

consist of a total of 116 (34) stations for precipitation (near-surface temperature), 44 (5) located in North, 55 (21) in Central, and 17 (7) in South Chile (see Figure 1). From Figure 1, we detected two relatively large strips where no instrumental records exist. The first, approximately between latitudes 24° and 27°S and a second between 34° and 35°S (34°–36°S for temperature). For the sake of clarity in the description of results, we therefore used those spatial gaps to define a northern region (~17°–24°S), a central region (~27°–34°S), and a southern region (~35°–40°S). Maximum elevations of the records of precipitation and temperature are, respectively 4,576 and 3,010 m in the north. For central, the highest altitude is 3,160 m and 1,043 m in the southern region.

Additionally, homogeneity in the annual series of precipitation and temperature was tested by Buishand's test (Buishand, 1982). The null hypothesis (H_0) for the tests is that data are independent, identically distributed random quantities, and the alternative (Ha) is that a change point in the mean (a break) is present. If such step cannot be determined in the time series data, the null hypothesis of homogeneity is not rejected. The null hypothesis was tested at 5% significance level. The test allowed identifying in-homogeneities in just 3 of the 91 precipitation time series from 1980 to 2015, and 5 of the 25 stations from 1990 to 2015. For temperature, 7 of the 23 stations from 1980 to 2015, and 2 of the 11 temperature time series from 1990 to 2015. These in-homogeneities were not corrected or discarded, but we have been checked that the main results are not altered by the inclusion of these stations (not showed).

2.2 | Gridded data sets

Five global gridded data sets were used—namely, (a) The Global Precipitation Climatology Project (GPCP) monthly analysis (New Version 2.3) provided by the National Oceanic and Atmospheric Administration (NOAA/OAR/ESRL PSD) (https://www.esrl.noaa.gov/psd/). The GPCP is a merger of various satellite-based rainfall estimates over both ocean and land, combined with the precipitation gauge analyses over land (Adler *et al*., 2003). (b) The Global Precipitation Climatology Centre (GPCC) Full Data Monthly Product Version 2018 (V8) available at https://www.esrl.noaa.gov/psd/. The GPCC product is based on in situ observations from rain gauges in order to provide gridded high-quality and high-resolution land surface precipitation analyses (Schneider *et al*., 2018). (c) Climatic Research Unit (CRU) time series version 4.01 available at http://badc.nerc.ac.uk/data/cru/. The CRU provides monthly mean precipitation and surface air temperature and merges observations at meteorological stations across land areas using angular distance weighting

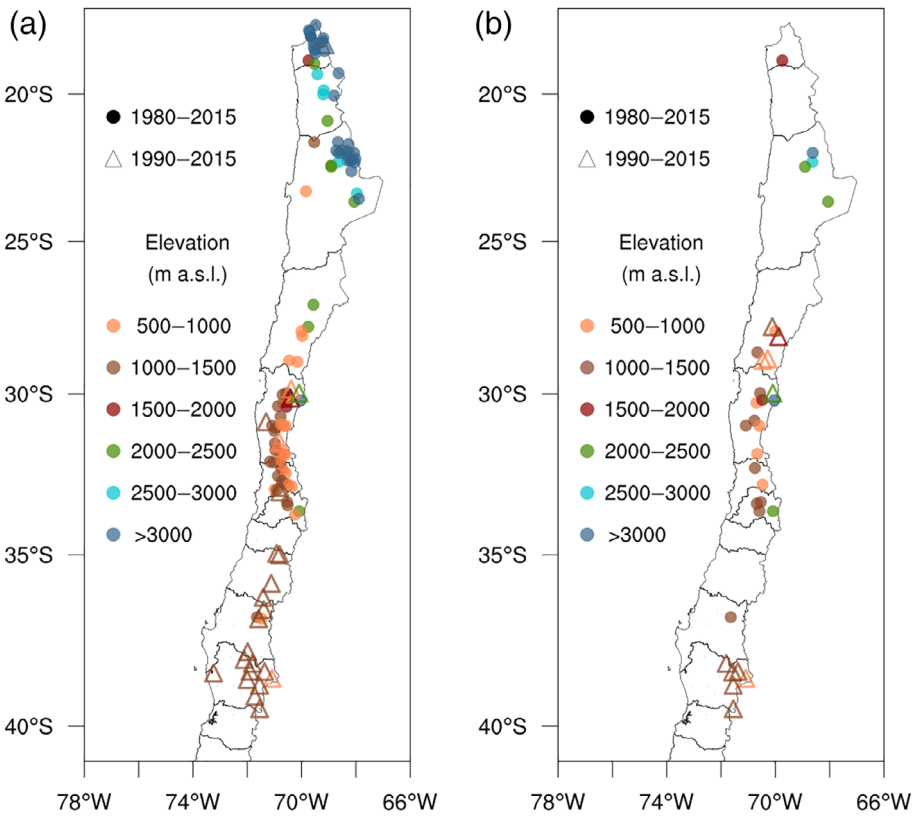

FIGURE 1 Location of the selected meteorological stations including time span (years) and its corresponding elevation for (a) precipitation and (b) temperature [Colour figure can be viewed at wileyonlinelibrary.com]

interpolation (Harris *et al*., 2014). CRU data set includes about 44 stations used in precipitation analysis, and no stations for temperature analysis. Both GPCC and CRU are based on ground stations, in addition to the difference in spatial resolution between them; the main sources used for construction are different. CRU is obtained through the national meteorological agencies (NMAs), the World Meteorological Organization (WMO), the Centro Internacional de Agricultura Tropical, the Food and Agriculture Organization (FAO) and others. GPCC includes NMAs, WMO, FAO, GHCN at the National Centers for Environmental Information, data collections from international regional projects, as well as the global data collections of the CRU (Sun *et al*., 2018). (d) Re-Analysis Interim Project (ERA-I), which is a global atmospheric reanalysis produced by the European Centre for Medium-Range Weather Forecasts (ECMWF) that can be accessed from https://apps.ecmwf.int/datasets/. The ERA-I is produced using a sequential 4D-VAR data assimilation scheme (Dee *et al*., 2011), and (e) Modern-Era Retrospective analysis for Research and Applications Version 2 (MERRA2). The MERRA2 is the newest reanalysis product from the NASA Global Modeling and Assimilation Office (GMAO), generated using the Goddard Earth Observing System Model, Version 5 data assimilation system (Bosilovich *et al*., 2017) available at https://gmao.gsfc.nasa.gov. Additional information of the gridded data sets is presented in Table 1. Further details about data assimilation techniques and physical processes represented in these data sets are summarized in Fujiwara *et al*. (2017).

2.3 | Methods

To compare the gridded data sets with observations, we interpolated the data sets (with simple bilinear interpolation) to the station location, to reduce the error in spatial position "and not to"overcome the mismatch in scale. The bilinear interpolation method uses the distance-weighted average of the four nearest grid values to give an estimate at a point of interest. This grid-to-point methodology has been applied satisfactorily in previous studies (e.g., Bromwich and Fogt, 2004; Bao and Zhang, 2013; Ebrahimi *et al*., 2017; Mayor *et al*., 2017; Meher and Das, 2019). The bilinear interpolation has been chosen due to its more realistic local interpretation instead of using the coarse grid value. This simplified method with two-dimensional interpolation allows assessing improvements and uncertainties (Uddin *et al*., 2008; Caroletti *et al*., 2019). An attempt of interpolation of the observations would involve large uncertainties given the lack of high-density weather stations database along the complex terrain (Rivera *et al*., 2018).

The evaluation of the gridded data sets to represent annual and seasonal features associated with precipitation and surface temperature over high Chilean Andes, included computation of several validation statistics: difference (bias), root mean square error (RSME), the Pearson correlation coefficient (CC), and Willmott index of agreement (Skill). The positive values of bias indicate an overestimation of the precipitation or temperature of the gridded data sets in relation to observed, whereas negative values indicate underestimation. The RSME provides information on the standard metric errors, where 0 is the best score. The CC indicates a linear relationship between the gridded data sets and observations, where 1 is the perfect match. Willmott's index is a standardized measure of the degree of data set temporal-prediction error and varies between 0 and 1, where value of 1 indicates a perfect match, and 0 indicates no agreement.

The Sen Slope and the Mann–Kendall test are used to estimate annual and seasonal trends in time series. Trends are considered to be statistically significant at the 10% significance level. A more detailed description of these methods can be found in Mann (1945), Kendall (1975) and Wilks (2006). The gridded data sets were compared for annual, summer (December–February, DJF) and winter (June–August, JJA) periods.

TABLE 1 Spatial horizontal resolution of the gridded data sets used in this study

Gridded data	Variables	Resolution	Description	References
GPCP	*P*	2.5°× 2.5°	Centre: GSFC NASA	Adler *et al*. (2003)
GPCC	*P*	1° × 1°	Centre: DWD	Schneider *et al*. (2018)
CRU	*P* and *T*	0.5° × 0.5°	Centre: UEA	Harris *et al*. (2014)
ERA-I	*P* and *T*	0.75° × 0.75°	Centre: ECMWF	Dee *et al*. (2011)
MERRA2	*P* and *T*	0.5° × 0.625°	Centre: NASA GMAO	Bosilovich *et al*. (2017)

Note: *P* indicates precipitation and *T* indicates temperature.

Abbreviations: CRU, Climatic Research Unit; ERA-I, Re-Analysis Interim Project; GPCC, Global Precipitation Climatology Centre; GPCP, Global Precipitation Climatology Project; MERRA2, Modern-Era Retrospective analysis for Research and Applications Version 2.

In order to explore the influence of climate indices onto precipitation and temperature variability, Pearson's correlation was performed between climate indices and the time series of observations and gridded data sets. The indices are: Niño 1.2 (0°–10°S; 90°–80°W) and Niño 3.4 (5°N–5°S; 170°–120°W), the Pacific Decadal Oscillation (PDO), and the Antarctic Oscillation (AAO). The time series of the climate indices are provided by the NOAA website (https://www.esrl.noaa.gov/psd/data/climateindices).

To further illustrate the representation of long-term trends associated with some precipitation and temperature extremes in the high Chilean Andes, daily precipitation/temperature data from station observation and gridded data sets (GPCP available from 1996 to 2015 at https://www.ncdc.noaa.gov/cdr/atmospheric, GPCC available from 1982 to 2015 at https://www.dwd.de/EN/ourservices/gpcc/gpcc.html, ERA-I and MERRA2) for annual and seasonal scales are used to analyze spatio-temporal trends of precipitation and surface temperature. For this, two precipitation-related indices were used: the maximum number of consecutive wet days (CWD) and consecutive dry days (CDD). The CWD is defined by the maximum length of wet spell (daily rainfall $\geq$1 mm) whereas CDD by the maximum length of dry spell (daily rainfall <1 mm). And two temperature-related indices: the number of warm days (TX90p) and cold days (TX10p). The TX90p is defined by the maximum length of warm spell (daily temperature > 90th percentile) whereas TX10p by the maximum length of cold spell (daily temperature < 10th percentile). Both indices expressed in days.

3 | RESULTS AND DISCUSSION

3.1 | Annual and seasonal precipitation analyses

The annual precipitation regime is characterized by a contrast among the three regions in Chile (Figure 2a). In the north, some records near the coast show annual precipitation lower than 10 mm·year^{-1}. These values contrast with increasing precipitation to the east, where the highest values are observed in the elevated areas (>3,000 m) (Figures 1c and 2a). This zonal gradient highlights the orographic precipitation over the windward slope (Garreaud *et al*., 2017).

There is also a clear latitudinal pattern of gradual increase of precipitation, with maximum annual mean precipitation concentrated southward to 35°S, with values above 1,000 mm. During summer, precipitation increases in northern and decreases in central region, whereas in winter, precipitation decreases in northern and an increase in central region (Figure 2b,c). The summer season is responsible for up to 80% of the rainfall occurring in the northern region, in contrasts with the central and the south regions, where about 40–80% of precipitation falls during the winter season.

Figures 3 and 4 are boxplots that summarize the overall performance of the gridded data sets in reproducing the annual and seasonal precipitation through the calculation of bias, RSME, CC and Skill. In Northern Chile, positive biases in GPCP and ERA-I indicate overestimate precipitation, whereas for GPCC, CRU and MERRA2 a median close to zero bias, although MERRA2 is slightly more negative. In central region, GPCC shows an improvement by lower median and quartile values. Southward 35°S, all data sets underestimate precipitation in relation to observations. It is worth mentioning that MERRA2 tends to be drier across the whole study area (Figure 3a–c); however, the median values of MERRA2 is almost the same as some of the other data sets.

All gridded data sets show smaller RSME in Northern and Central Chile, on the other hand, a larger RSME is noted in Southern Chile (Figure 3d–f). In general, GPCC and CRU match observations in the north, with median and quartile values smaller than 10 mm·year^{-1}, while GPCC and ERA-I perform better in the south, with median values smaller than 100 mm·year^{-1}. The data sets do a good job in central region, with smaller bias as well as RSME values. Most of the data sets show a high correlation, with CC values greater than 0.8, particularly in central region. MERRA2 shows poor agreement compared to other data sets due to extreme negative bias values. The good agreement in Central Chile is also shown by the Skill index between gridded data sets and observations, particularly by CRU in North and Central Chile (Figure 3j,k). On the other hand, lower Skill index is reported for all data sets in the south. Both north and central regions have relatively low biases, however, in the arid north, the agreement with observations by CC and Skill is generally low; this might be related to the inherent dynamics of precipitation in the region: rainfall usually occurs as a few extreme events (e.g., Pendergrass and Knutti, 2018; Meseguer-Ruiz *et al*., 2019), which are more difficult to reproduce.

Figure 4 depicts seasonal precipitation statistics between gridded data sets and observations for summer and winter. In summer, gridded data sets reproduce similar annual bias variability in North and Southern Chile; however, biases are higher in the northern region and lower in the south. Differences between data sets are noted in central region, where all data sets appear to be positively biased relative to observations. GPCP and ERA-I overestimate precipitation with maximum values

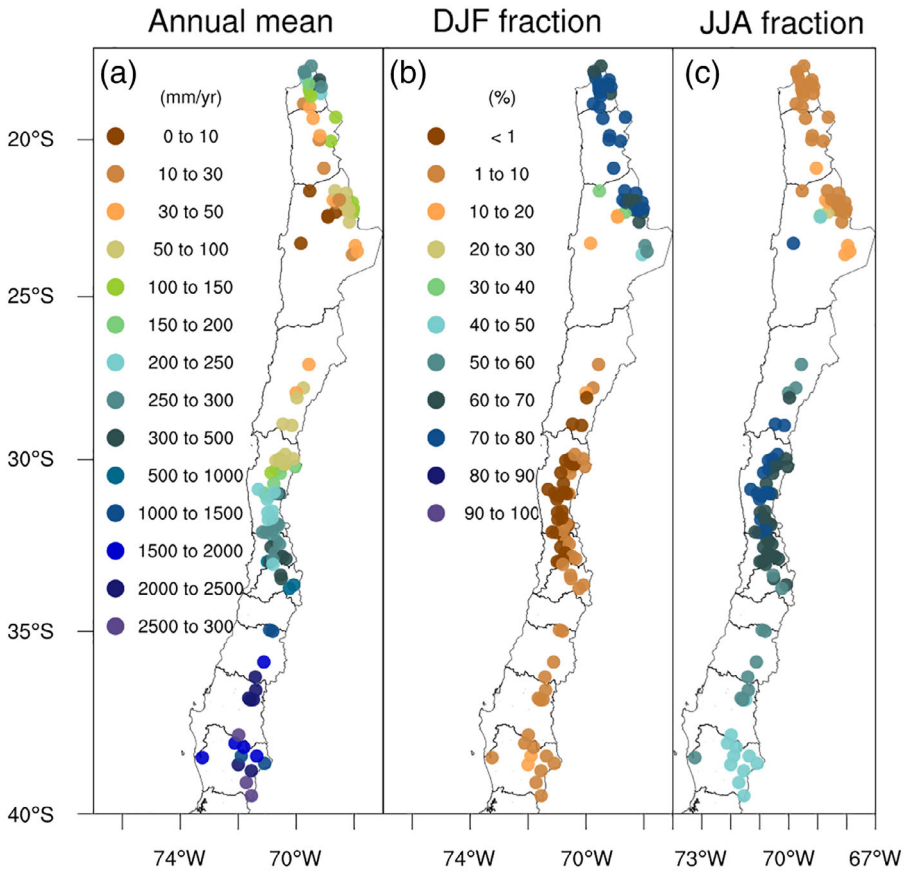

FIGURE 2 (a) Spatial distribution of the annual mean accumulation of precipitation. (b) Summer (DJF) fraction of the annual total and (c) winter (JJA) fraction of the annual total. DJF, December–February; JJA, June–August [Colour figure can be viewed at wileyonlinelibrary.com]

above 15 mm, whereas GPCC, CRU and MERRA2 show smaller bias (Figure 4b). Concerning winter precipitation bias, once again GPCC, CRU and MERRA2 close match with observations, depict smaller biases in Northern Chile. In central region, variability of gridded data sets is similar to what already seen for annual bias, with ERA-I and GPCP overestimating precipitation (Figure 4n), and southward 35°S all gridded data sets underestimate observed precipitation (Figure 4c–o).

For RSME, larger values are found in northern and southern regions during summer, while in winter large disagreement occurs over central and the southern regions (Figure 4e,f,q,r). In northern region, GPCC and CRU (GPCC and MERRA2) have a smaller RSME, <30 mm·year^{-1}. (<5 mm·year^{-1}, quartile and median values) in summer (winter), whereas, about median values, all data sets, except ERA-I, have a RMSE <30 mm·year^{-1}. In general, the errors associated with each gridded data set are accompanied by the magnitude of bias; the larger (lower) the bias, the greater (lower) the error in relation to the observations. In terms of the bias and RSME values, GPCC and CRU show the best performance.

The values of CC and Skill index show a better agreement between gridded data sets and observations in Northern Chile during summer (less spread), except to MERRA2. Maximum CC values are delivered by CRU in all regions. For Central Chile, GPCC and CRU have a good agreement, and GPCC and ERA-I for Southern Chile (Figure 4g–l). In winter, the CC and Skill show that all data sets provide a good agreement to observed precipitation over central region. Conversely, poor performances are delivered in Southern Chile in line with strong negative correlation (Figure 4u,z).

Analysis of the performance of gridded data sets reproducing the annual and seasonal precipitation shows that GPCP and ERA-I overestimate observations in the north, while MERRA2 underestimates the annual as well as seasonal precipitation. Better match is given in Central Chile (27°–34°S) with higher CC, Skill and smaller bias. However, in general, the data sets are very close when comparing the median per region and season.

It can be argued that in northern region, differences among the data sets are related to orographic forcing processes, whereas changes in the south (35°–40°S) may be induced by differences in meso-scale processes, such as the maritime advection of water vapor, as well as the performance of each data to reproduce the strength and frequency of cold frontal systems (Barrett *et al.*, 2009). As discussed by Justino *et al.* (2011) and Van den Broeke *et al.* (2005), misrepresentation of regions with steep slopes modifies the wind pattern, changing the temperature and consequently resulting in unrealistic contrast.

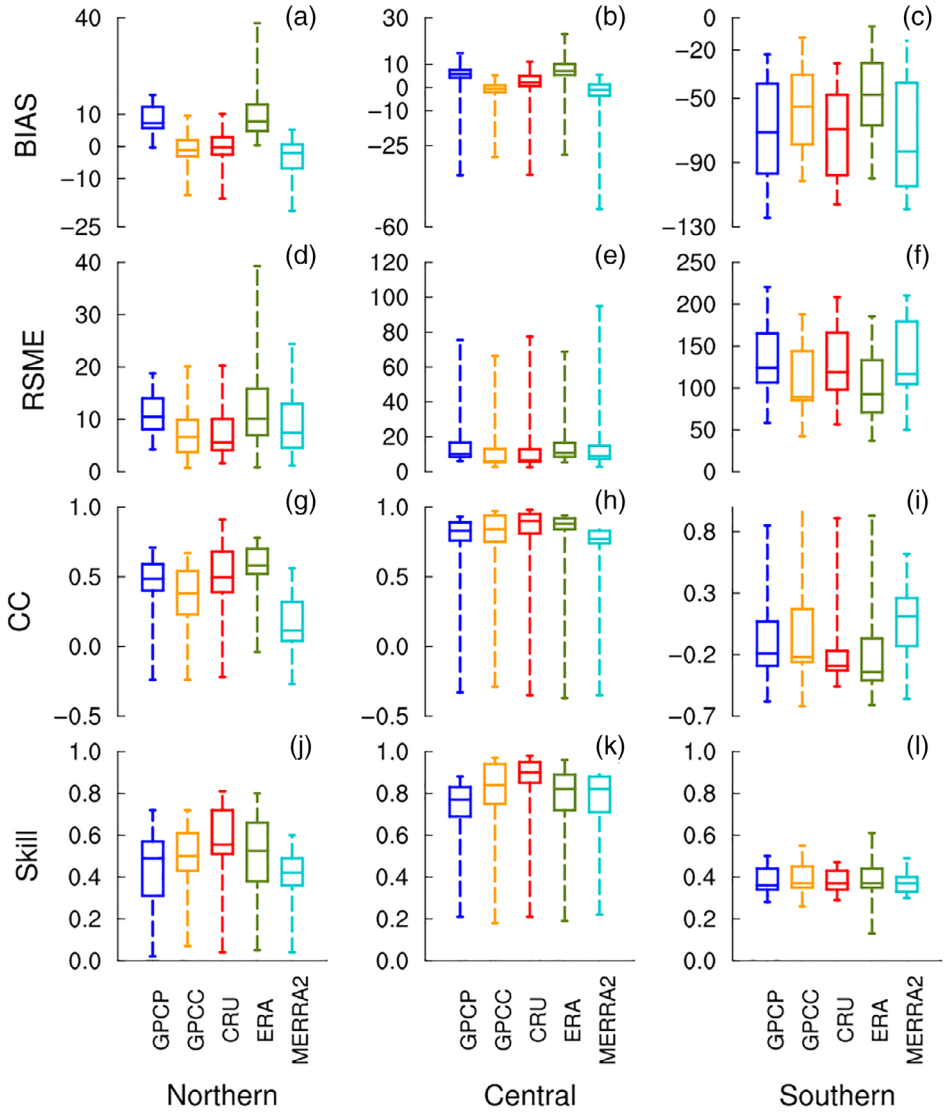

FIGURE 3 Distribution of bias (mm·year^{-1}) (a–c), RSME (mm·year^{-1}) (d–f), CC (g–i) and Willmott's index of agreement (Skill) (j–l) of annual accumulation precipitation. The line in the Box represents the median (50%), the bottom and top of the box represent the first (25%) and third (75%) quartiles, the whiskers indicate variability outside the lower and upper quartiles. Note that axis range for bias, RSME and CC differs in each panel. CC, correlation coefficient; RSME, root mean square error [Colour figure can be viewed at wileyonlinelibrary.com]

It can be argued that GPCC and CRU reasonably reproduce the annual and seasonal mean precipitation in most parts of the studied region, as they are based on in situ rainfall observation data. The CRU data are interpolated directly from station observations, including algorithms that account for the effect of elevation (New *et al*., 2000). Conversely, GPCP is less skilled reproducing instrumental precipitation over steep terrain and high elevation due to its relatively coarse resolution, despite merging observation and satellite data. It is also possible that satellites cannot capture key processes. GPCP relies on passive microwave and infrared retrievals of precipitation, which are unable to represent an orographic enhancement. These differences between gridded products suggest that higher horizontal resolution results in more accurate representation in this complex Andean terrain (Figure 1c). However, it is important to note that these data sets may perform better when compared with observations in flatter terrain below our 500-m altitude criteria.

3.2 | Annual and seasonal precipitation trends

Station observations show that negative trends in annual total precipitation are widespread in the Central and South Chile (Figure 5a). This is consistent with earlier findings of Quintana (2012). Few exceptions are observed in Northern Chile, with negative trends in high altitudes and positive or no trends in low altitudes, which 20% of trends are statistically significant and 59.5% nonsignificant.

The number of observations that have no trends are dominant between 21° and 34°S in the summer season, and during winter northward to 25°S (Figure 5f,k). Nonsignificant positive trends are observed, northward to

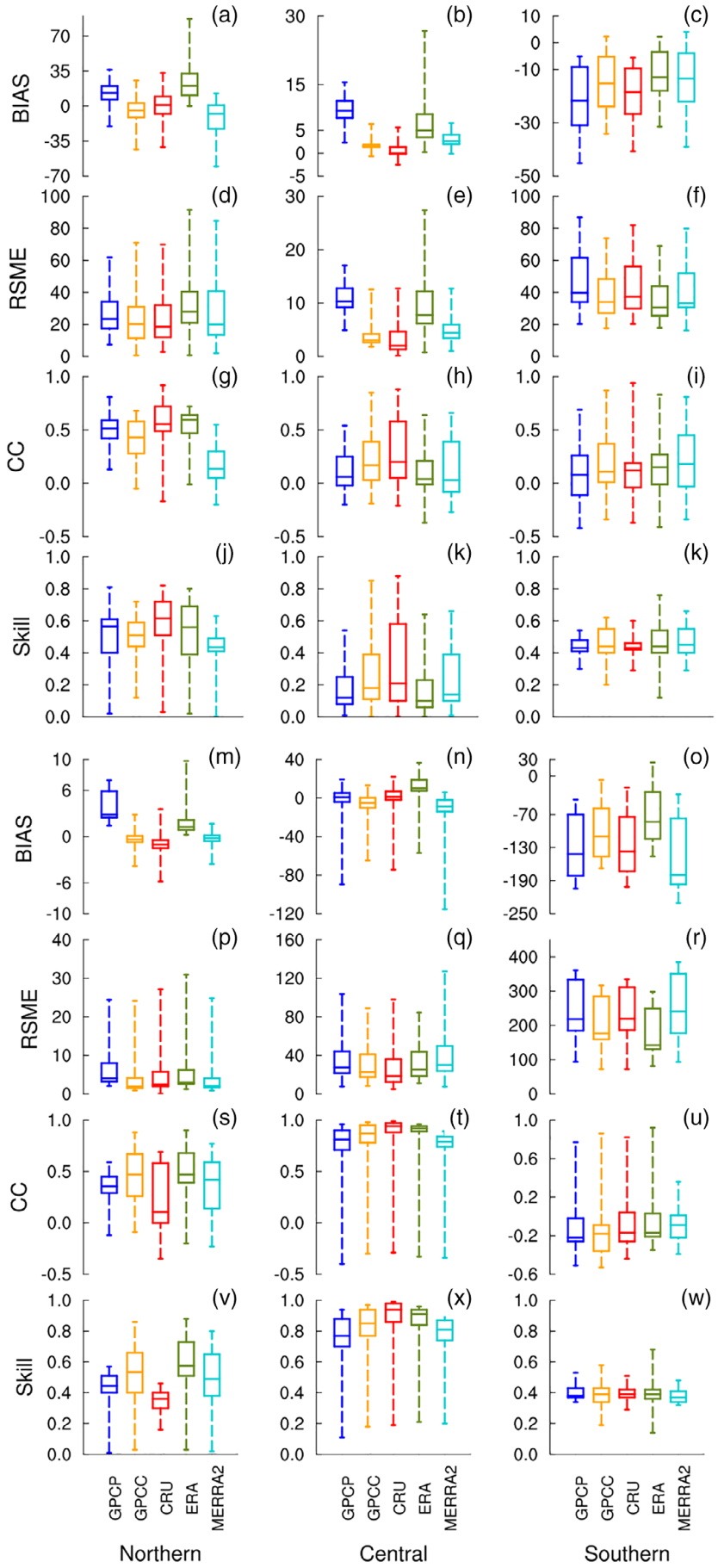

FIGURE 4 As Figure 3, but for summer (DJF) (a–l) and winter (JJA) (m–w) precipitation [Colour figure can be viewed at wileyonlinelibrary.com]

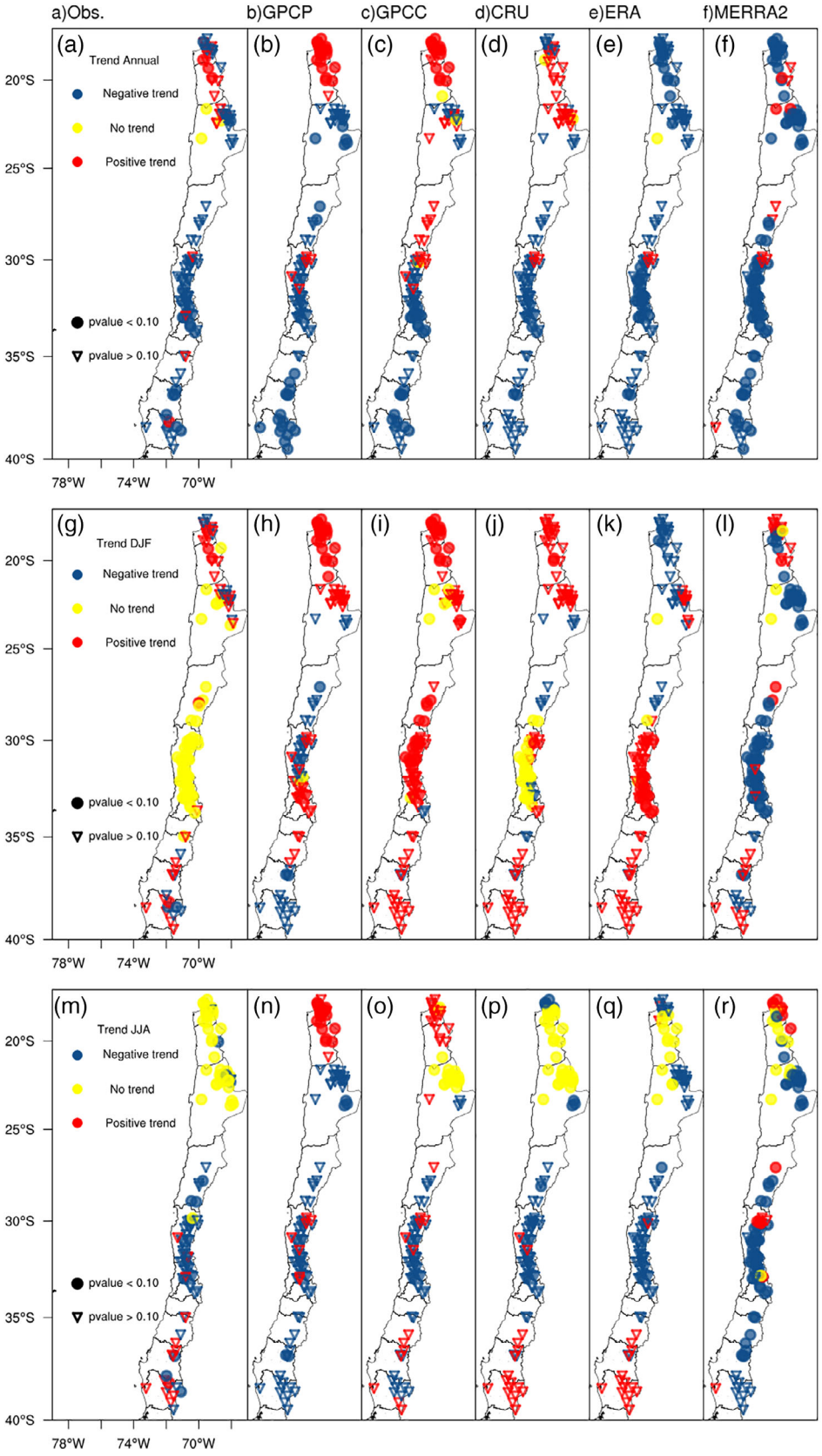

FIGURE 5 Annual and seasonal trend of precipitation from stations observations and gridded data. The _lled circles are related to statistically signi_cant trends at the 10% level [Colour figure can be viewed at wileyonlinelibrary.com]

21°S and southward to 36°S during the summer season, whereas in winter there are positive trends southward to 35°S. These positive nonsignificant trends for summer and winter may be associated with the increase of extreme rainfall events (Pfahl *et al.*, 2017). However, observed negative trend signal during winter corresponds

TABLE 2 Correlation coefficients between time series of annual and seasonal precipitation from observed and gridded data sets with climate indices

		Niño1.2			Niño3.4			PDO			AAO		
Data	**Season**	**N**	**C**	**S**	**N**	**C**	**S**	**N**	**C**	**S**	**N**	**C**	**S**
Obs.	Annual	−0.11	**0.49**	0.13	−0.17	**0.53**	**0.46**	−0.15	**0.30***	0.12	0.1	−0.19	−0.23
	DJF	**−0.29**	**0.35**	−0.15	**−0.49**	**0.33**	**−0.45**	−0.15	−0.02	**−0.27***	−0.2	0.14	**0.48**
	JJA	**0.34**	**0.45**	0.19	**0.42**	**0.60**	**0.34**	**0.36**	0.26	0.11	0.13	−0.09	−0.26
	Annual	−0.11	**0.40**	0.18	−0.18	**0.44***	**0.45**	−0.01	0.23	**0.37**	0.08	−0.25	**−0.45***
GPCP	DJF	**−0.39**	0.14	−0.09	**−0.40**	0.12	0.12	0.11	0.13	−0.07	0.11	−0.39	**−0.33**
	JJA	**0.32***	**0.35**	0.13	**0.39**	**0.53**	**0.30***	0.22	0.16	**0.39**	0.16	−0.08	−0.02
	Annual	−0.18	**0.44**	0.19	−0.26	**0.49**	**0.44**	−0.09	**0.29***	**0.27***	0.19	**−0.28***	**−0.40**
GPCC	DJF	**−0.3**6	−0.04	−0.18	**−0.45**	−0.09	−0.01	0.05	**−0.30***	−0.24	**0.08**	0.13	−0.13
	JJA	**0.25**	**0.40**	0.14	**0.46**	**0.57**	0.24	0.24	0.22	**0.28***	0.15	−0.08	0.01
	Annual	−0.12	**0.47**	0.21	−0.09	**0.49**	**0.47**	−0.15	**0.29***	0.18	0.03	−0.25	**−0.33**
CRU	DJF	−0.27	0.23	−0.18	**−0.40**	0.14	−0.02	−0.15	0.16	**−0.27***	0.14	−0.26	**−0.18**
	JJA	**0.41**	**0.46**	0.26	**0.51**	**0.60**	**0.31***	0.07	0.25	0.19	0.02	−0.08	−0.01
	Annual	−0.08	**0.44**	0.13	−0.03	**0.46**	**0.38**	0.02	**0.32***	0.25	0.08	−0.26	**−0.40**
ERA	DJF	**−0.35**	−0.05	−0.06	**−0.44**	−0.20	0.08	0.03	−0.33	−0.19	0.06	−0.06	**−0.06**
	JJA	0.23	**0.42**	0.15	**0.41**	**0.53**	0.21	**0.28***	**0.32***	0.22	0.06	−0.05	0.01
	Annual	−0.09	**0.35**	0.13	0.06	**0.46**	**0.34**	0.13	**0.30***	**0.33**	−0.25	**−0.34**	**−0.32***
MERRA2	DJF	−0.16	−0.01	−0.19	−0.13	−0.05	−0.04	0.14	−0.14	−0.25	**0.37**	**0.34**	**−0.13**
	JJA	**0.28***	**0.29***	0.17	**0.37**	**0.54**	0.20	0.17	0.27	**0.36**	−0.06	−0.12	0.01

Note: Columns are organized according to northern (N), central (C) and southern (S) regions. Bold numbers indicate statistically significant correlations at the 5% level and bold with asterisks are significant at the 10% level.

Abbreviations: CRU, Climatic Research Unit; DJF, December–February; ERA, Re-Analysis Interim Project; GPCC, Global Precipitation Climatology Centre; GPCP, Global Precipitation Climatology Project; JJA, June–August.

to 53% of the stations, which 14% are significant (Figure 5m). This is consistent with previous drought linked to decreasing frequency of winter precipitation in this region (Boisier *et al*., 2016; Garreaud *et al*., 2017; Polade *et al*., 2017).

Annual precipitation trends delivered by gridded data sets show good agreement with the observed pattern, with frequent negative trends throughout the region (Figure 5b–f). Southward 25°S, all data sets indicate reduction in precipitation. A slightly less coherent pattern is detected in northern, where GPCP, GPCC and CRU present some locations with positive trends, opposite to the corresponding station observations. This likely comes from the effect of precipitation trends delivered by both data sets for summer (Figure 5k,l). Between 27° and 35°S the annual trend is a response to winter conditions because no trends are detected in summer from observations and also delivered by CRU. In the southernmost part of the region, there is no dominant season (DJF, JJA) in the annual trend. It is important to note that the dry bias delivered by MERRA2 results in a negative trend in both summer and winter conditions (Figure 5l,r).

3.3 | Relationship of precipitation and climate indices

For station, observed precipitation time series shows significant positive correlations with El Niño 1.2 and El Niño 3.4 indices, particularly in central region, in both seasons (Table 2). The precipitation pattern in Northern Chile is not affected by El Niño Southern Oscillation (ENSO) at the annual scale. On the other hand, seasonal precipitation presents a strong relationship with ENSO in Northern Chile, with negative (positive) significant correlation in summer (winter). A similar response is also detected in the southern region in relation to Niño 3.4. It is well known that El Niño events induce wet (dry) conditions in Central Chile in winter (summer), associated with northward migration (southern permanency) of subtropical anticyclone (Montecinos and Aceituno, 2003; Valdés-Pineda *et al*., 2016).

Observations are more closely related to the El Niño 3.4 index, with statistically significant higher correlations (positive correlations) ranging from to 0.33 to 0.60. The influence of the PDO and AAO is less noticeable, except

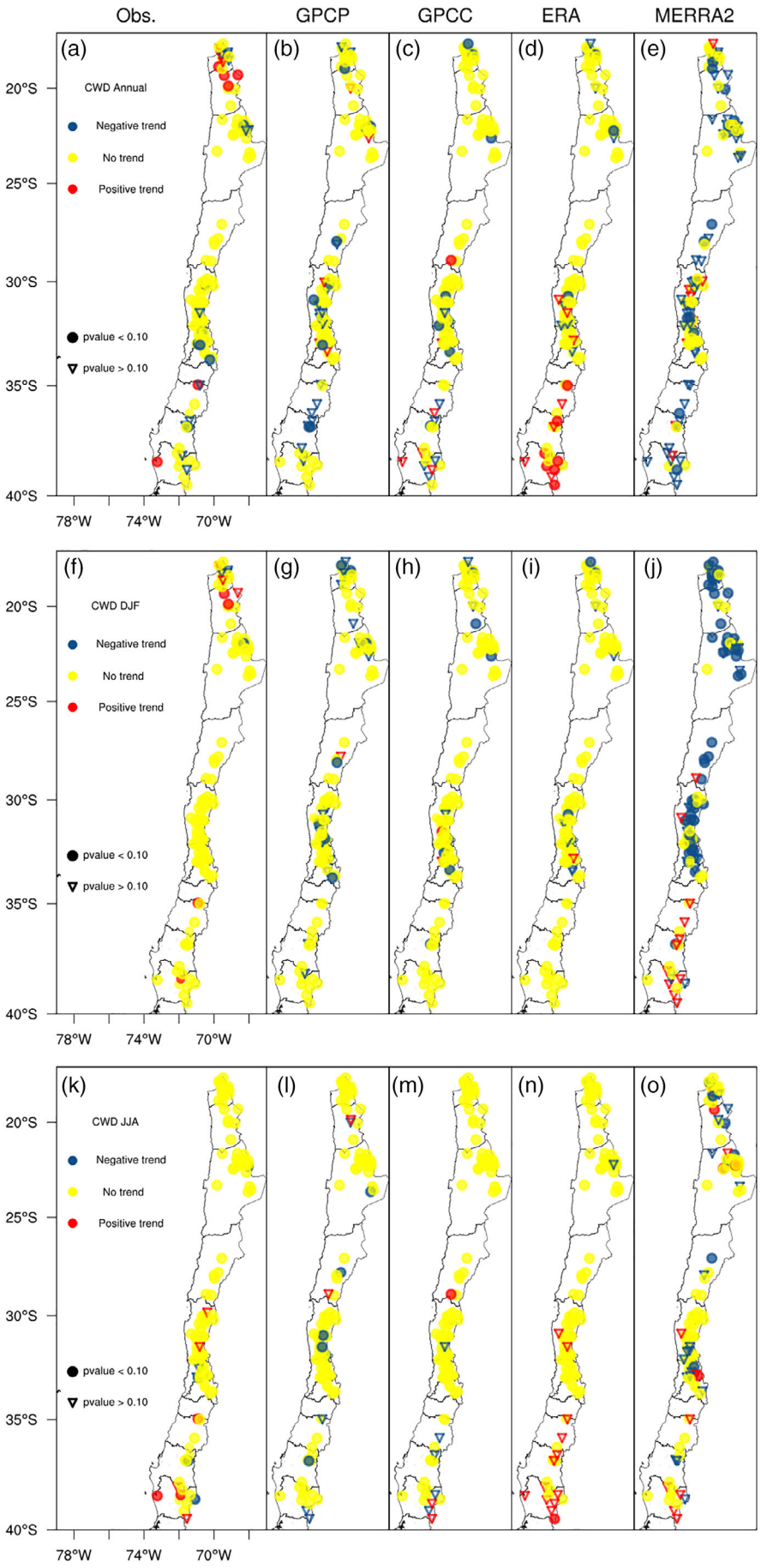

FIGURE 6 As Figure 5, but for annual and seasonal maximum number of consecutive wet days (CWD) [Colour figure can be viewed at wileyonlinelibrary.com]

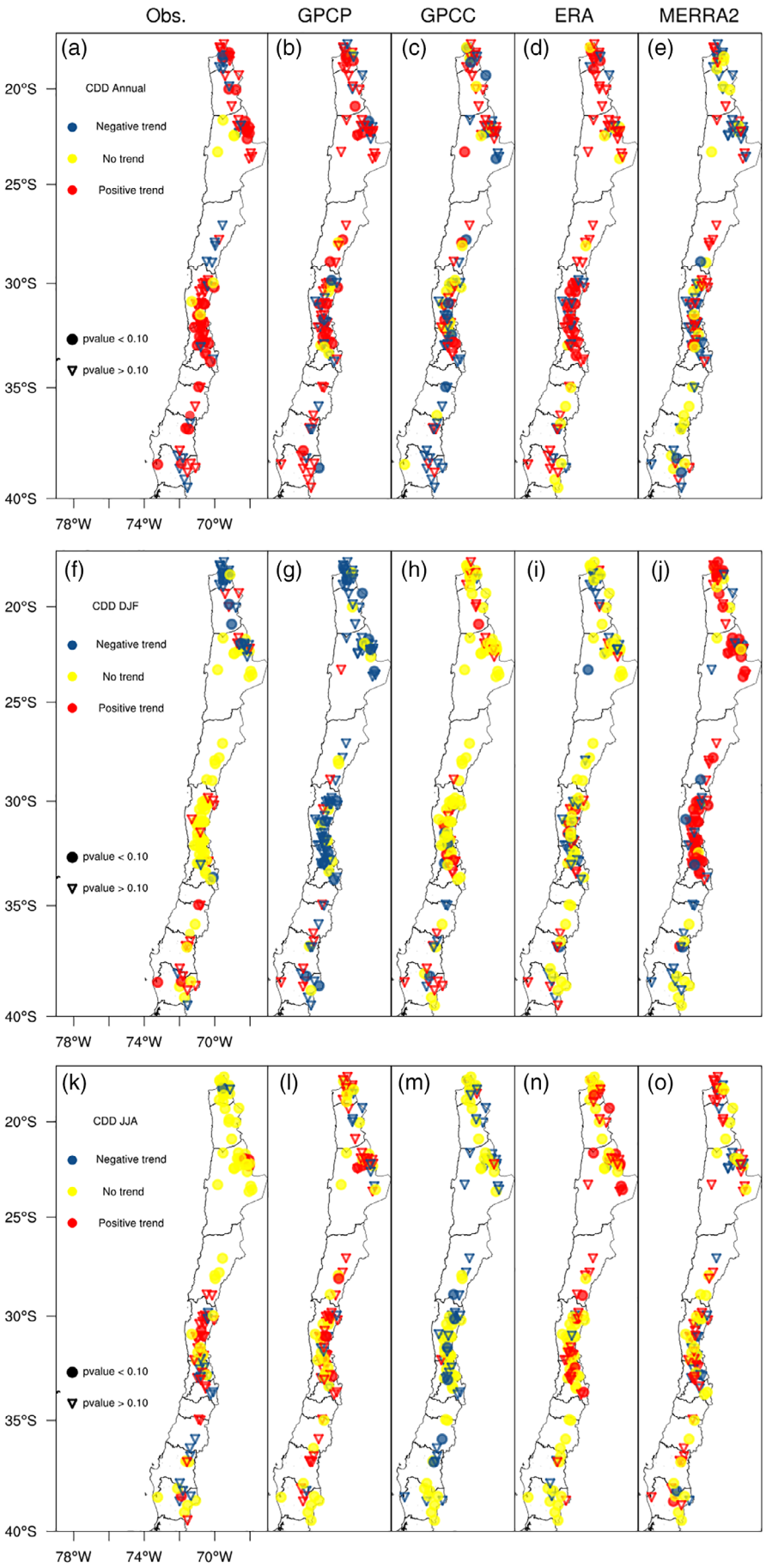

FIGURE 7 As Figure 5, but for annual and seasonal maximum number of consecutive dry days (CDD) [Colour figure can be viewed at wileyonlinelibrary.com]

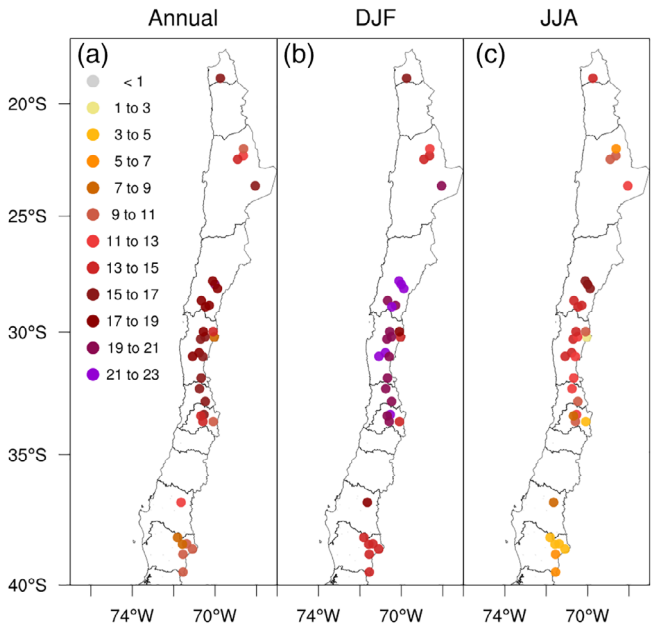

FIGURE 8 Spatial distribution of the annual and seasonal mean temperature from weather station observations [Colour figure can be viewed at wileyonlinelibrary.com]

for annual and winter precipitation. The AAO index is significant in the south region with correlation by up to 0.48 during summer.

The correlation based on gridded data sets shows a different pattern for both indices (ENSO, AAO and PDO) as compared to observations. The main differences between gridded data sets and observations are link to the signal of the correlation. For ENSO indices, GPCC, CRU and ERA-I are able to mimic the correlation signal described based on instrumental observations. Table 2 shows significant values for CRU in JJA for Niño 1.2 and Niño 3.4, and in DJF for Niño 3.4, for ERA in DJF for Niño 1.2 and Niño 3.4, and in JJA for Niño 3.4.

The MERRA2 and GPCP show positive significant correlations during winter (JJA) in Northern and Central Chile, with both ENSO indices. In contrast to observed data, gridded data sets do not show any significant correlations between summer precipitation and ENSO indices over Central Chile. Regarding the PDO and AAO, best correlations for the gridded data sets relative to the stations data are found for the annual and summer seasons for all study areas.

3.4 | Extreme precipitation indices

Figure 6 shows the trend in CWD for each station and for each corresponding time series derived from the gridded data sets. Neither instrumental observations nor gridded data sets show significant trends in CWD for annual and seasonal level (Figure 6), except for some significant positive trends over Northern Chile in the annual scale. Conversely, MERRA2 presents some negative trends in several locations. Turning to annual CDD shows general significant positive trends over the entire study area concerning to station observations (Figure 7). This pattern is well reproduced by GPCP and ERA-I, while GPCC and MERRA2 have slightly more negative or no trends. Observations deliver by about 81% of the stations have positive trends, of which 28.5% are statistically significant. Insofar as gridded data sets are concerned, GPCP shows 75% of positive trends, GPCC with 59%, ERA-I 84%, and MERRA2 with 54%.

On the other hand, CDD during summer conditions show negative trends in Northern Chile, standing out as the only region with some detectable trends (22.5%) (Figure 7f). GPCP delivers a widespread negative trend whereas MERRA2 shows positive trends in most locations during the summer season. In winter, observations and almost all gridded data sets show no change of precipitation in northern region, conversely, positive trend is found in Central Chile, except for GPCC. About 83% of stations deliver positive trends (8% statistically significant), followed by GPCP with 87%, 54% for GPCC, 94% ERA-I and MERRA2 with 77%. These changes agree with the findings of others studies with the increasing of CDD in Chile (e.g., Henríquez *et al*., 2019).

3.5 | Annual and seasonal temperature analyses

Figure 8 shows the distribution of annual and seasonal mean surface temperature based on observations. The mean annual temperature varies between 9 and 19°C. Higher temperature values occur in Central Chile, between 27° and 34°S. Mean summer temperatures within the altitudinal range considered in our study can reach up to 23°C. In winter, temperature fluctuates around 12°C, southward to 35°S; the values are lower and range between 3 and 7°C. In northern region (17°–24°S) temperature presents lower seasonal variability, with differences between summer and winter by about 4 and 8°C, varying with altitude.

Comparison between gridded data sets and observations for annual surface temperature is shown in Figure 9. There is an overall cold bias in the whole region, but more noticeable within in Central Chile. In the north, smaller bias is depicted by MERRA2, with median values close to zero and an interquartile range between 0 and −2°C (Figure 9a). In Central Chile,

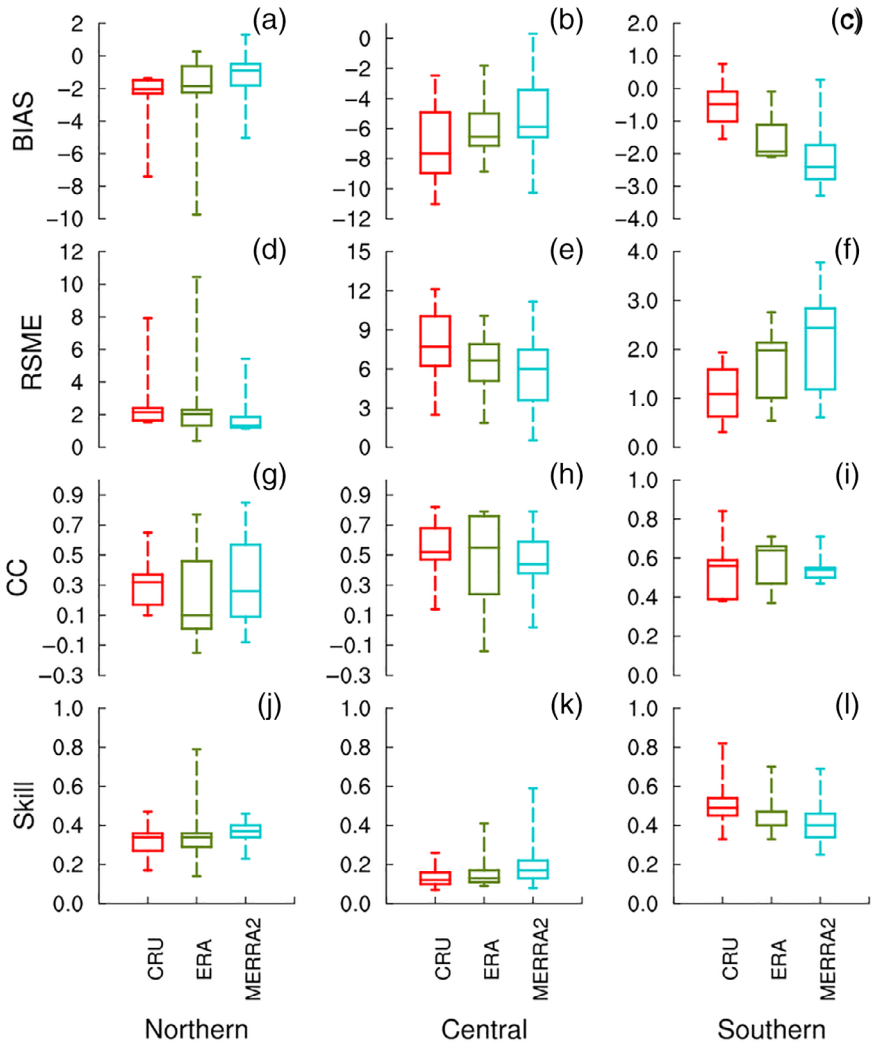

FIGURE 9 Distribution of bias (oC·year^{-1}) (a–c), RSME (oC·year^{-1}) (d–f), CC (g–i) and Willmott's index of agreement (Skill) (j–l) of annual mean temperature. The line in the Box represents the median (50%), the bottom and top of the Box represent the first (25%) and third (75%) quartiles, the whiskers indicate variability outside the lower and upper quartiles. Note that axis range for bias, RSME and CC di_ers in each panel. CC, correlation coefficient; RSME, root mean square error [Colour figure can be viewed at wileyonlinelibrary.com]

MERRA2 also exhibits smaller bias followed by ERA-I and CRU. On the other hand, Southern Chile presents an inverse pattern with CRU having smaller bias and MERRA2 greater variability (Figure 9c). Data sets with large biases tend to show by high RSME (Figure 9d–f). Correlation analyses and the Skill index show a good agreement between the data sets.

As in the case for annual comparisons, seasonal disaggregation indicates a cold bias in summer and winter in all gridded data sets along this high Andean region, except for CRU in Southern Chile during summer (Figure 10c). Evaluation for RSME shows similar values in summer as well as in winter, with large bias paired with high RSME. The bias, RSME, CC and Skill values show that all data sets provide a good approximation to observed surface temperature over Northern Chile during summer, and Northern and Southern Chile in winter. In general, MERRA2 matches closely with observations in Northern and Central Chile, while CRU has a good performs in Southern Chile.

3.6 | Annual and seasonal temperature trends

Figure 11a shows the trends in annual mean surface temperature for station observations. Results indicate that with few exceptions, there are significant positive trends in the mean annual surface temperature. The warming trends correspond to about 79% of observations, where 38% are statistically significant, with a maximum magnitude of 0.68°C·decade^{-1} in Northern Chile, and 0.43°C·decade^{-1} in Central Chile. It is important to note that although 41% of the other stations do not show statistically significant changes, they are dominated by positive trends as well.

Significant warming trends are also identified in summer (71% of stations) and winter (65% of stations) with a positive trend signal. About 26.5 and 20.5% are statistically significant trends for summer and winter observations (Figure 11e,i). This is consistent with earlier findings for northern region (Meseguer-Ruiz *et al*., 2018)

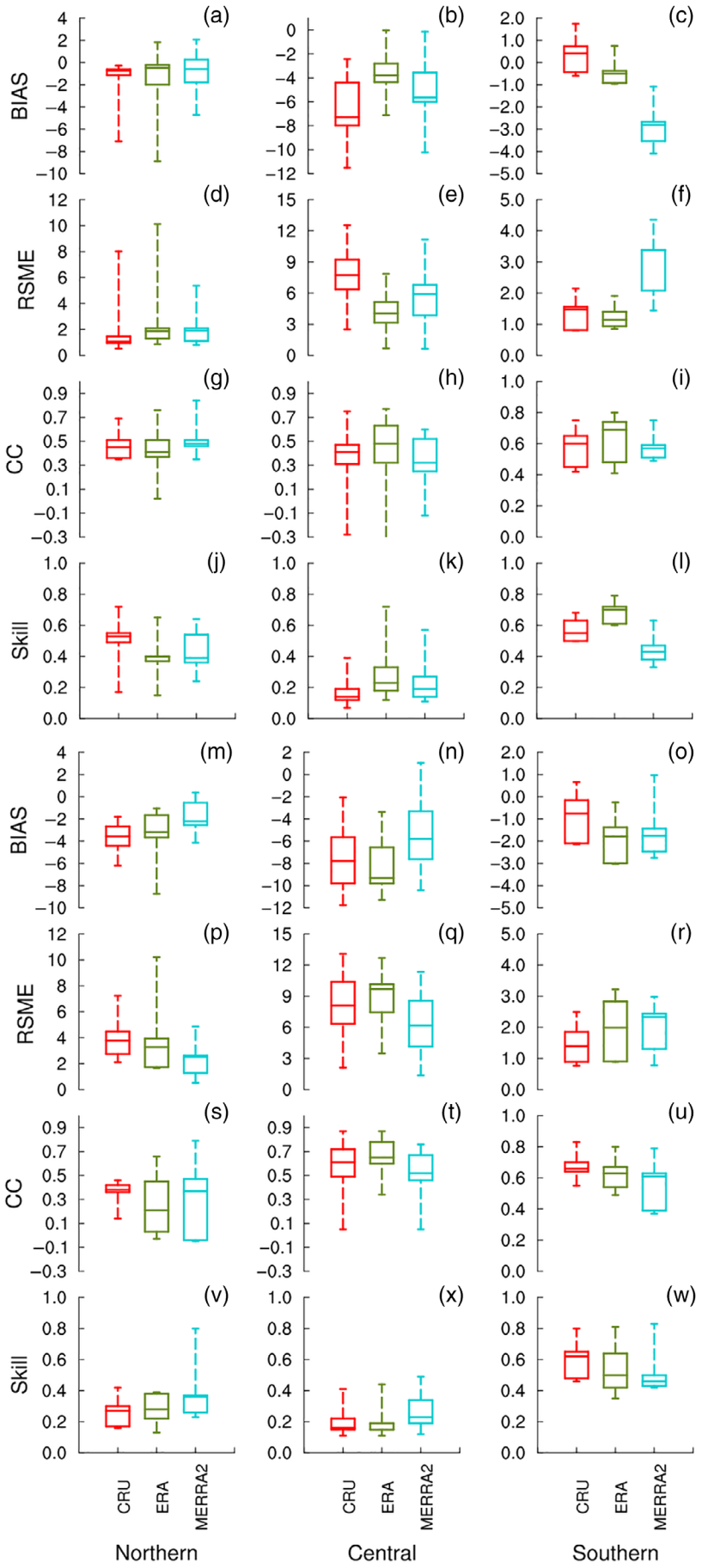

FIGURE 10 As Figure 9, but for summer (DJF) (a–l) and winter (JJA) (m–w) temperature. DJF, December–February; JJA, June–August [Colour figure can be viewed at wileyonlinelibrary.com]

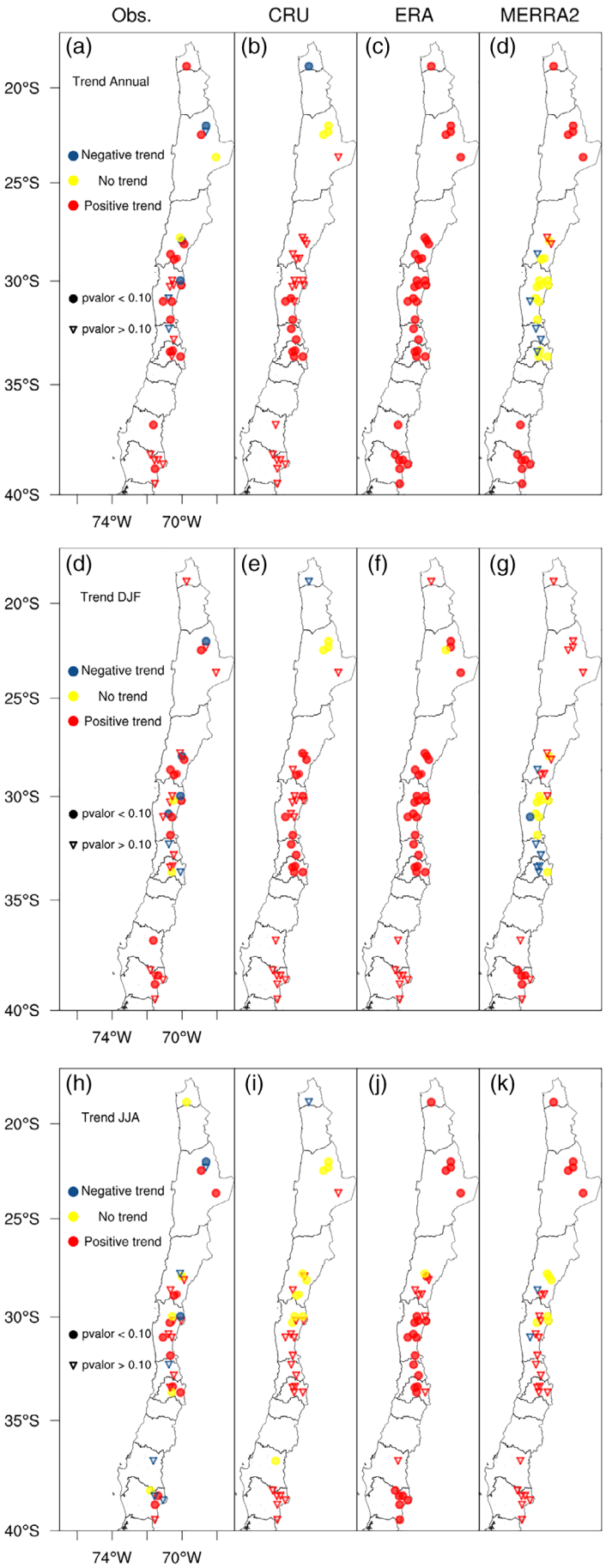

FIGURE 11 Annual and seasonal trend of temperature from stations observations and gridded data. The _lled circles are related to statistically signi_cant trends at the 10% level [Colour figure can be viewed at wileyonlinelibrary.com]

TABLE 3 Correlation coefficients between observed and gridded datA sets of annual and seasonal temperature with climate indices

		Niño1.2		Niño3.4			PDO			AAO			
Data	**Season**	**N**	**C**	**S**	**N**	**C**	**S**	**N**	**C**	**S**	**N**	**C**	**S**
Obs.	Annual	**0.45**	0.09	**0.28***	**0.56**	**0.35**	0.2	0.15	−0.04	−0.005	0.11	0.09	0.2
	DJF	**0.53**	0.13	−0.13	**0.65**	0.11	−0.22	0.23	0.11	−0.15	0.08	0.01	−0.1
	JJA	**0.35**	−0.06	0.13	**0.40**	**0.27***	0.24	0.12	−0.07	0.11	−0.04	0.02	0.2
	Annual	**0.80**	**0.30***	**0.35**	**0.81**	**0.45**	0.24	**0.46**	0.21	0.014	0.09	0.23	0.19
CRU	DJF	**0.70**	−0.01	−0.06	**0.60**	−0.03	−0.19	**0.28***	0.14	−0.22	0.09	−0.01	0.03
	JJA	**0.65**	0.21	0.16	**0.65**	**0.46**	0.27	0.43	0.15	0.12	0.05	0.03	0.17
	Annual	**0.33**	0.07	0.23	**0.47**	0.21	0.13	0.03	−0.2	−0.16	0.11	0.12	0.15
ERA	DJF	**0.65**	0.16	−0.06	**0.66**	0.15	−0.14	0.15	0.1	−0.19	0.04	−0.09	−0.03
	JJA	**0.29***	−0.06	0.1	**0.36**	0.27	0.23	−0.05	−0.06	−0.015	−0.05	0.008	0.15
	Annual	**0.34**	−0.05	0.11	**0.52**	0.12	−0.04	0.17	0.28	0.23	**0.31***	**0.34**	0.26
MERRA2	DJF	**0.70**	0.19	−0.13	**0.70**	**0.28***	−0.22	**0.28***	**0.54**	−0.06	−0.16	−0.08	−0.02
	JJA	0.18	−0.19	0.05	**0.45**	0.07	0.05	0.02	0.09	0.26	−0.03	0.05	0.14

Note: Columns are organized according to northern (N), central (C) and southern (S) regions. Bold numbers indicate statistically significant correlations at the 5% level and bold with asterisks are significant at the 10% level.

Abbreviations: CRU, Climatic Research Unit; DJF, December–February; ERA, Re-Analysis Interim Project; GPCC, Global Precipitation Climatology Centre; GPCP, Global Precipitation Climatology Project; JJA, June–August.

as well as for Central Chile (Burger *et al*., 2018), suggesting the end of the regional cooling trend that occurred between 1979 and 2006. This cooling trend was related to negative phase of the Interdecadal Pacific Oscillation (IPO), allowing widespread warming trends associated with an increase of sea surface temperature.

Patterns of annual and seasonal variability from gridded data sets are similar to instrumental observations pattern, with dominance of positive trends. Annual and summer temperature trends diverge over central part of the studied region where MERRA2 displays more stations with no trend compared to the other data sets (Figure 11d,h). In contrast, statistically significant upward trends predominate in ERA-I. During winter season, there is an increase in the number of stations that do not experience trends, in particular CRU and MERRA2.

3.7 | Temperature and climate indices

Table 3 shows the temporal correlation between annual and seasonal temperatures and climate indices. El Niño 1.2 has a strong correlation with the observed annual surface temperature pattern in Northern Chile, the El Niño 3.4 correlation is lower for Central and Southern Chile.

This agreement between temperature and ENSO indices in northern region is captured by all gridded data sets, except for MERRA2 for El Niño 1.2 during winter. It should be mentioned that correlations shown by CRU in Central Chile exhibit a similar behavior as those calculated from observations. Annual and seasonal observed temperature do not correlate with neither PDO nor AAO. ERA-I replicates this behavior for these climate modes. Conversely, CRU presents a positive correlation with PDO, and MERRA2 with PDO and AAO in Northern and Central Chile.

3.8 | Extreme temperature indices

Figure 12 shows the trend in TX90p for each station and for each corresponding time series derived from the gridded data sets. In general, no trends are found for the annual scale from station observations (42% of stations) except for some specific stations, mainly located in the central region, with positive trend. Widespread no trend is depicted by ERA-I and MERRA2. On contrary, negative nonsignificant trends are noted in almost Chile (52% of stations) from station observations during summer season, however, in the central region some stations do not show a trend signal, while others point to a statistically significant positive trend. ERA-I shows a negative trend throughout Chile, on the other hand, MERRA2 shows a generalized pattern without trend, except for some exception in the central region (positive trend) (Figure 12d,e). Turning to winter season, TX90p shows general positive trends over the entire study area concerning to station observations (76% of stations), while ERA-I and MERRA 2 show different contrasts between themselves and the observations.

About the TX10p at annual scale, similar pattern with the TX90p is show from station observation and

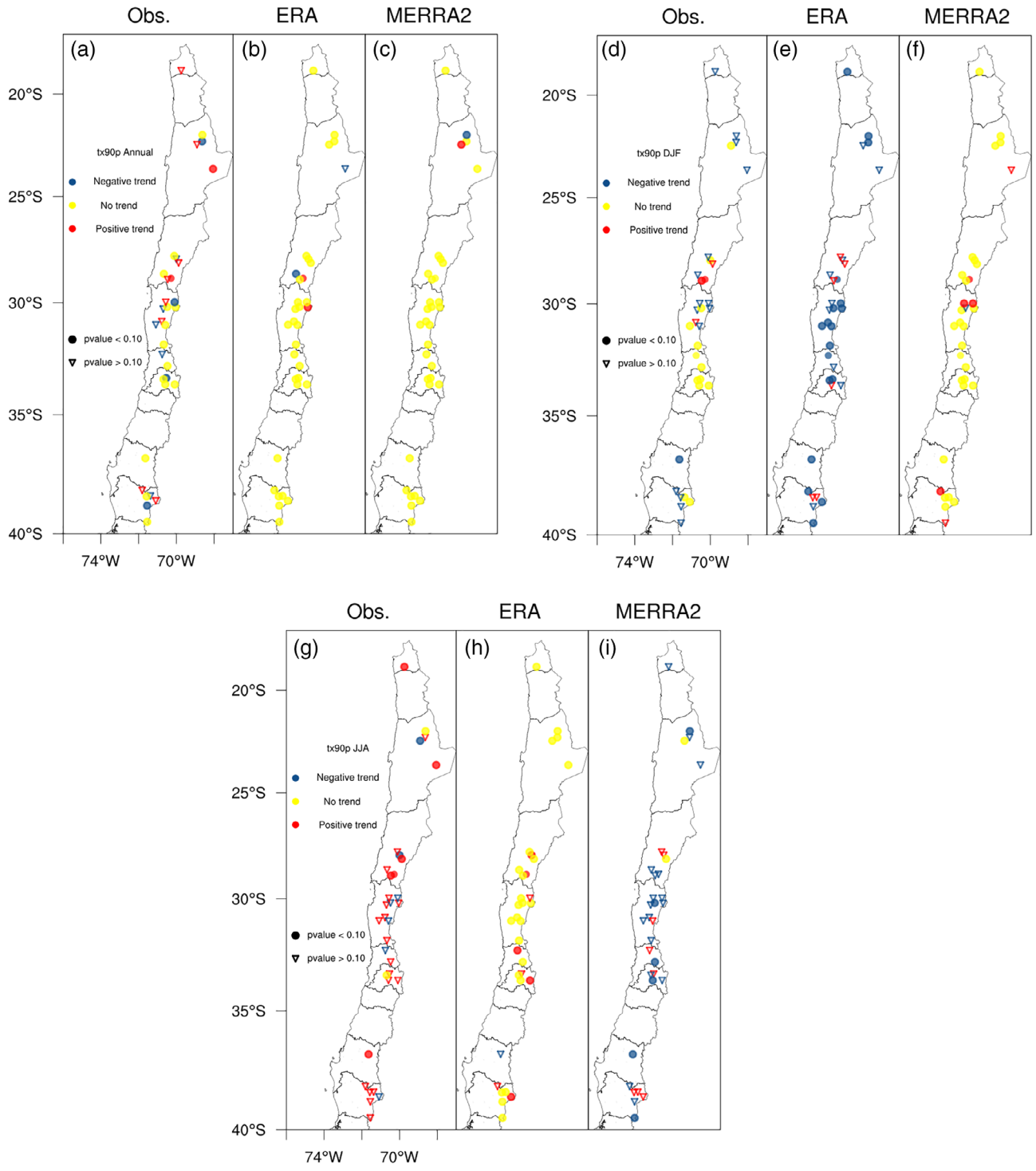

FIGURE 12 As Figure 11, but for annual and seasonal number of warm days (TX90p) [Colour figure can be viewed at wileyonlinelibrary.com]

gridded data sets (Figure 13a–c). On the other hand, about 70% of stations show a positive trend from station observation during the summer season. A similar pattern is depicted by MERRA2, with 58% of stations point to a positive trend, whereas ERA-I shows only 30% of stations. For the winter season, the trend signal of observations is more widespread, with 48% of the season showing a negative trend, 45% no trend and 21% a positive trend, more concentrated in Central Chile (Figure 13g–i).

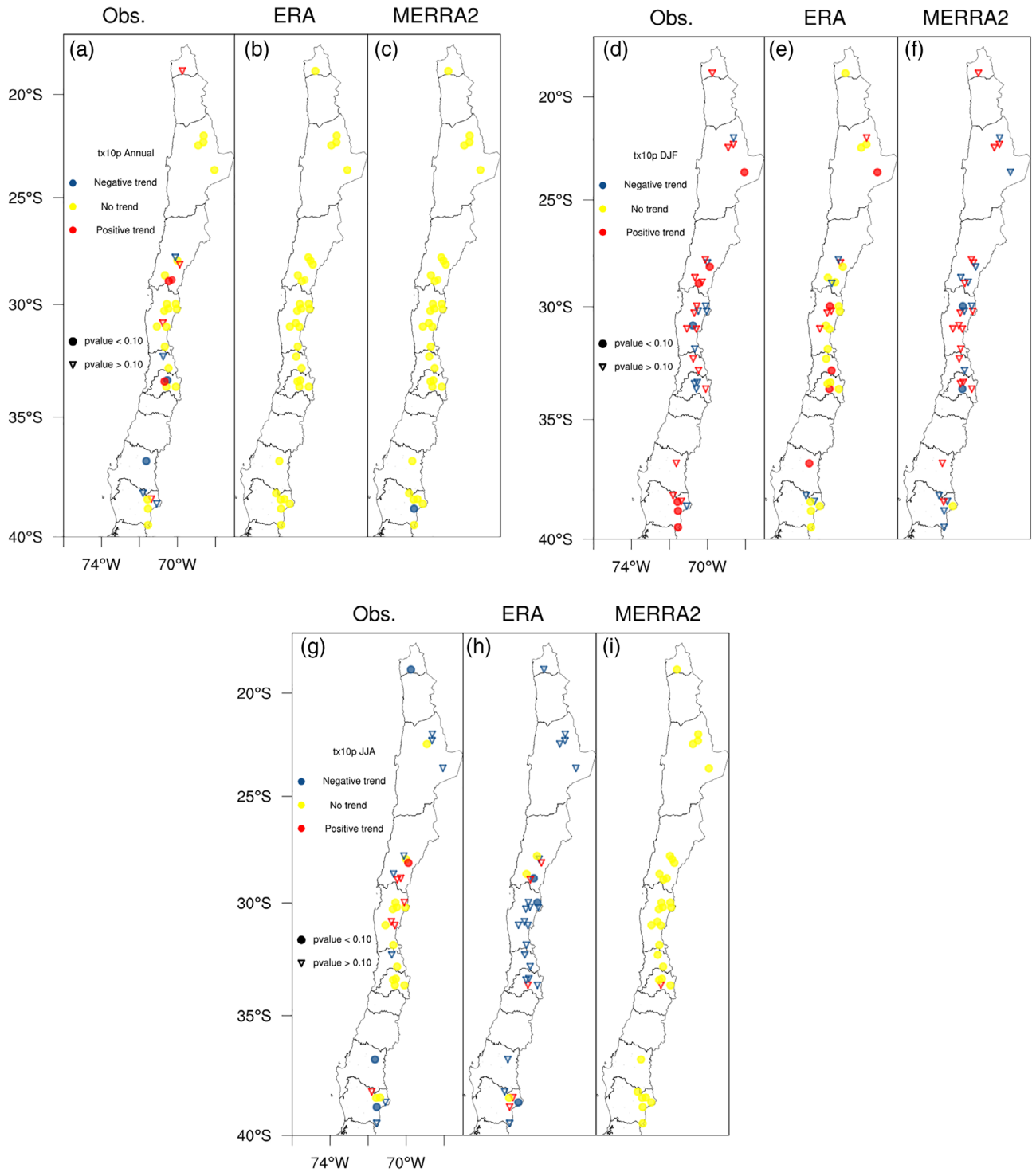

FIGURE 13 As Figure 11, but for annual and seasonal number of cold days (TX10p) [Colour figure can be viewed at wileyonlinelibrary.com]

4 | CONCLUSIONS

In this study, we have evaluated the performance of five gridded data sets in reproducing the observed annual and seasonal mean precipitation, and surface temperature over Northern, Central and Southern over Chilean Andes. In addition, long-term trends are also analyzed with focus on high-elevated areas from station observations and gridded data sets.

The ability of gridded data sets to represent the observed precipitation as well as temperature is variable, in part due to their coarse spatial resolution leading to

misrepresentation of the complex topography in Chilean Andes. Weaker performance was shown by GPCP very likely related to coarsest spatial resolution compared to other data sets. However, a coarser grid cell does not always translate into good or poor performance. For instance, GPCC superior performance in precipitation achieved with only 1° grid-cell size, contrasts with the lower skill of MERRA2 with a relatively fine spatial resolution (0.5°). This is important to mention that we are evaluating global gridded data sets in which they are designed to perform well over large areas; however, the add value and performance of these data sets may be more outstanding than regional reanalysis (e.g., Kaiser-Weiss *et al.*, 2019).

The results demonstrated that the performance of each data sets varies on the Andean regions analyzed, fluctuating on overestimating or underestimating the precipitation and temperature. It has been demonstrated that there are several differences between gridded data sets and station observations. These differences are larger in Northern Chile (17°–24°S) and southward of 35°S in relation to total precipitation, whereas for surface temperature disagreement is higher in Central Chile, between 27° and 35°S. In general, good performance is achieved by CRU, GPCC and ERA-I in most precipitation analyses, whereas CRU and ERA-I do a good job for temperature analyses. It is important to mention that the number of stations located in Chile (and surroundings) that goes into the gridded data set will have a large influence too. MERRA2 tends to underestimate precipitation and temperature mainly in the central and southern regions, leading to greater mismatches with observation, and greater disagreement in trend analysis.

It has also been investigated correlations between climate indices with precipitation and temperature patterns. The response of precipitation to ENSO based on gridded data sets are consistent in the sense that higher significant correlations occur in Central Chile, being related to the regions with higher number of observations. Additional to ENSO, this region is also affected by PDO, with good agreement between observed and gridded data sets. Our analysis also showed that the AAO plays a role in summer precipitation in Southern Chile. On the other hand, surface temperature depicted by observed and gridded data sets are strongly correlated with ENSO in northern sector, while PDO and AAO indices do not seem to related with temperature, except by for CRU and MERRA2 in north and central regions.

Our work evidences a significant reduction of annual precipitation and warming trends in the high Chilean Andes during the study period. Station observations and most of gridded data sets show a decrease of winter precipitation, especially in Central Chile, as well as an increase of the consecutive number of dry days is detected in annually in all regions on this study, particularly in Central Chile during winter season. Additionally, an increase of warm days is observed mainly during the winter season. This combination of increased temperature and reduced precipitation may contribute to intensification of extreme dry events in arid areas, critically affecting the current availability of water resources in Chile. Moreover, if these changes in temperature and precipitation continue, these can pose a serious threat to the stability of the glaciers due to mass imbalance.

ACKNOWLEDGEMENTS

The authors want to thank the Coordination for the Improvement of Higher Education Personnel (CAPES), CNPq 306181-20169 and FAPEMIG PPM00773-18. FONDECYT Project 11160059 from the Chilean Government. A.F.'s work is funded by FONDECYT 11160454 and 1171065.

ORCID

Vanúcia Schumacher https://orcid.org/0000-0003-1753-567X
Alfonso Fernández https://orcid.org/0000-0001-6825-0426
Oliver Meseguer-Ruiz https://orcid.org/0000-0002-2222-6137
Alcimoni Comin https://orcid.org/0000-0002-8566-3254

REFERENCES

Adler, R.F., Huffman, G.J., Chang, A., Ferraro, R., Xie, P.-P., Janowiak, J., Rudolf, B., Schneider, U., Curtis, S., Bolvin, D., Gruber, A., Susskind, J., Arkin, P. and Nelkin, E. (2003) The Version-2 Global Precipitation Climatology Project (GPCP) monthly precipitation analysis (1979–present). *J Hydrometeorol*, 4, 1147–1167.

Alvarez-Garreton, C., Mendoza, P.A., Boisier, J.P., Addor, N., Galleguillos, M., Zambrano-Bigiarini, M. and Ayala, A. (2018) The CAMELS-CL dataset: catchment attributes and meteorology for large sample studies-Chile dataset. *Hydrology and Earth System Sciences*, 22(11), 5817–5846.

Angélil, O., Perkins-Kirkpatrick, S., Alexander, L.V., Stone, D., Donat, M.G., Wehner, M., Shiogama, H., Ciavarella, A. and Christidis, N. (2016) Comparing regional precipitation and temperature extremes in climate model and reanalysis products. *Weather Clim Extrem*, 13, 35–43.

Bao, X. and Zhang, F. (2013) Evaluation of NCEP–CFSR, NCEP–NCAR, ERA-Interim, and ERA-40 reanalysis datasets against independent sounding observations over the Tibetan Plateau. *Journal of Climate*, 26(1), 206–214.

Barrett, B.S., Garreaud, R. and Falvey, M. (2009) Effect of the Andes Cordillera on precipitation from a midlatitude cold front. *Monthly Weather Review*, 137, 3092–3109.

Bieniek, P.A., Bhatt, U.S., Walsh, J.E., Rupp, T.S., Zhang, J., Krieger, J. R. and Lader, R. (2016) Full access dynamical downscaling of ERA-interim temperature and precipitation for Alaska. *Journal of Applied Meteorology and Climatology*, 55, 635–654.

Blacutt, L.A., Herdies, D.L., de Gonçalves, L.G.G., Vila, D.A. and Andrade, M. (2015) Precipitation comparison for the CFSR, MERRA, TRMM3B42 and combined scheme datasets in Bolivia. *Atmospheric Research*, 163, 117–131.

Boisier, J.P., Rondanelli, R., Garreaud, R.D. and Muñoz, F. (2016) Anthropogenic and natural contributions to the Southeast Pacific precipitation decline and recent megadrought in central Chile. *Geophysical Research Letters*, 43, 413–421.

Bosilovich, M.G., Robertson, F.R., Takacs, L., Molod, A. and Mocko, D. (2017) Atmospheric water balance and variability in the MERRA-2 reanalysis. *Journal of Climate*, 30, 1177–1196.

Bradley, R.S. (2006) Climate change: threats to water supplies in the Tropical Andes. *Science (80-)*, 312, 1755–1756.

Bromwich, D.H. and Fogt, R.L. (2004) Strong trends in the skill of the ERA-40 and NCEP–NCAR reanalyses in the high and mid-latitudes of the Southern Hemisphere, 1958–2001. *Journal of Climate*, 17(23), 4603–4619.

Bromwich, D.H., Nicolas, J.P. and Monaghan, A.J. (2011) An assessment of precipitation changes over Antarctica and the southern ocean since 1989 in contemporary global reanalyses. *Journal of Climate*, 24, 4189–4209.

Buishand, T.A. (1982) Some methods for testing the homogeneity of rainfall records. *Journal of Hydrology*, 58, 11–27.

Burger, F., Brock, B. and Montecinos, A. (2018) Seasonal and elevational contrasts in temperature trends in Central Chile between 1979 and 2015. *Glob Planet Change*, 162, 136–147.

Caroletti, G.N., Coscarelli, R. and Caloiero, T. (2019) Validation of satellite, reanalysis and RCM data of monthly rainfall in Calabria (Southern Italy). *Remote Sensing*, 11(13), 1625.

Comin, A.N., Schumacher, V., Justino, F. and Fernández, A. (2018) Impact of different microphysical parameterizations on extreme snowfall events in the Southern Andes. *Weather Climate Extremes*, 21, 65–75.

Cortés, G., Girotto, M. and Margulis, S. (2016) Snow process estimation over the extratropical Andes using a data assimilation framework integrating MERRA data and Landsat imagery. *Water Resources Research*, 52, 2582–2600.

Cowtan, K. and Way, R.G. (2014) Coverage bias in the HadCRUT4 temperature series and its impact on recent temperature trends. *Quarterly Journal of the Royal Meteorological Society*, 140, 1935–1944.

Dee, D.P., Uppala, S.M., Simmons, A.J., Berrisford, P., Poli, P., Kobayashi, S., Andrae, U., Balmaseda, M.A., Balsamo, G., Bauer, P., Bechtold, P., Beljaars, A.C.M., Van de Berg, L., Bidlot, J., Bormann, N., Delsol, C., Dragani, R., Fuentes, M., Geer, A.J., Haimberger, L., Healy, S.B., Hersbach, H., Hólm, E. V., Isaksen, L., Kållberg, P., Köhler, M., Matricardi, M., Mcnally, A.P., Monge-Sanz, B.M., Morcrette, J.J., Park, B.K., Peubey, C., de Rosnay, P., Tavolato, C., Thépaut, J.N. and Vitart, F. (2011) The ERA-interim reanalysis: Configuration and performance of the data assimilation system. *Quarterly Journal of the Royal Meteorological Society*, 137, 553–597.

Ebrahimi, S., Chen, C., Chen, Q., Zhang, Y., Ma, N. and Zaman, Q. (2017) Effects of temporal scales and space mismatches on the TRMM 3B42 v7 precipitation product in a remote mountainous area. *Hydrological Processes*, 31(24), 4315–4327.

El-Samra, R., Bou-Zeid, E., Bangalath, H.K., Stenchikov, G. and El-Fadel, M. (2017) Future intensification of hydro-meteorological extremes: downscaling using the weather research and forecasting model. *Climate Dynamics*, 49, 3765–3785.

Fernández, A. and Mark, B.G. (2016) Modeling modern glacier response to climate changes along the Andes Cordillera: a multiscale review. *Journal of Advances in Modeling Earth Systems*, 8, 467–495.

Fujiwara, M., Wright, J.S., Manney, G.L., Gray, L.J., Anstey, J., Birner, T., Davis, S., Gerber, E.P., Lynn Harvey, V., Hegglin, M. I., Homeyer, C.R., Knox, J.A., Krüger, K., Lambert, A., Long, C. S., Martineau, P., Molod, A., Monge-Sanz, B.M., Santee, M.L., Tegtmeier, S., Chabrillat, S., Tan, D.G.H., Jackson, D.R., Polavarapu, S., Compo, G.P., Dragani, R., Ebisuzaki, W., Harada, Y., Kobayashi, C., McCarty, W., Onogi, K., Pawson, S., Simmons, A., Wargan, K., Whitaker, J.S. and Zou, C.Z. (2017) Introduction to the SPARC Reanalysis Intercomparison Project (S-RIP) and overview of the reanalysis systems. *Atmospheric Chemistry and Physics*, 17, 1417–1452.

Garreaud, R.D. (2009) The Andes climate and weather. *Advances in Geosciences*, 22, 3–11.

Garreaud, R.D., Alvarez-Garreton, C., Barichivich, J., Pablo Boisier, J., Christie, D., Galleguillos, M., LeQuesne, C., McPhee, J. and Zambrano-Bigiarini, M. (2017) The 2010-2015 megadrought in central Chile: impacts on regional hydroclimate and vegetation. *Hydrology and Earth System Sciences*, 21, 6307–6327.

Gu, G. and Adler, R.F. (2019) Precipitation, temperature, and moisture transport variations associated with two distinct ENSO flavors during 1979–2014. *Climate Dynamics*, 52, 7249–7265.

Harris, I., Jones, P.D., Osborn, T.J. and Lister, D.H. (2014) Updated high-resolution grids of monthly climatic observations—the CRU TS3.10 dataset. *International Journal of Climatology*, 34, 623–642.

Henríquez, C., Qüense, J., Villarroel, C. and Mallea, C. (2019) 50-Years of climate extreme indices trends and inventory of natural disasters in Chilean cities (1965–2015). In: *Urban Climates in Latin America*. Cham: Springer, pp. 281–308.

Huang, D.Q., Zhu, J., Zhang, Y.C., Huang, Y. and Kuang, X.Y. (2016) Assessment of summer monsoon precipitation derived from five reanalysis datasets over East Asia. *Quarterly Journal of the Royal Meteorological Society*, 142, 108–119.

Justino, F., Setzer, A., Bracegirdle, T.J., Mendes, D., Grimm, A., Dechiche, G. and Schaefer, C.E.G.R. (2011) Harmonic analysis of climatological temperature over Antarctica: Present day and greenhouse warming perspectives. *International Journal of Climatology*, 31, 514–530.

Kaiser-Weiss, A.K., Borsche, M., Niermann, D., Kaspar, F., Lussana, C., Isotta, F.A. and Undén, P. (2019) Added value of regional reanalyses for climatological applications. *Environmental Research Communications*, 1(7), 071004.

Kendall, M. (1975) *Rank Correlation Methods*. London: Charles Griffin.

Lorenz, C. and Kunstmann, H. (2012) The hydrological cycle in three state-of-the-art reanalyses: Intercomparison and performance analysis. *Journal of Hydrometeorology*, 13, 1397–1420.

Mann, H.B. (1945) Nonparametric tests against trend econometrica, 13, 245–259.

Manz, B., Buytaert, W., Zulkafli, Z., Lavado, W., Willems, B., Robles, L.A. and Rodríguez-Sánchez, J.P. (2016) High-resolution satellite-gauge merged precipitation climatologies of the Tropical Andes. *Journal of Geophysical Research – Atmospheres*, 121, 1190–1207.

Masiokas, M.H., Villalba, R., Christie, D.A., Betman, E., Luckman, B.H., Le Quesne, C., Prieto, M.R. and Mauget, S. (2012) Snowpack variations since AD 1150 in the Andes of Chile and Argentina (30°–37°S) inferred from rainfall, tree-ring and documentary records. *Journal of Geophysical Research – Atmospheres*, 117, 1–11.

Mayor, Y., Tereshchenko, I., Fonseca-Hernández, M., Pantoja, D. and Montes, J. (2017) Evaluation of error in IMERG precipitation estimates under different topographic conditions and temporal scales over Mexico. *Remote Sensing*, 9(5), 503.

Meher, J.K. and Das, L. (2019) Gridded data as a source of missing data replacement in station records. *Journal of Earth System Science*, 128(3), 58.

Meseguer-Ruiz, O., Ponce-Philimon, P.I., Guijarro, J.A. and Sarricolea, P. (2019) Spatial distribution and trends of different precipitation variability indices based on daily data in Northern Chile between 1966 and 2015. *International Journal of Climatology*, 39, 4595–4610.

Meseguer-Ruiz, O., Ponce-Philimon, P.I., Quispe-Jofré, A.S., Guijarro, J.A. and Sarricolea, P. (2018) Spatial behavior of daily observed extreme temperatures in Northern Chile (1966–2015): data quality, warming trends, and its orographic and latitudinal effects. *Stochastic Environmental Research and Risk Assessment*, 6, 1–21.

Montecinos, A. and Aceituno, P. (2003) Seasonality of the ENSO-related rainfall variability in central Chile and associated circulation anomalies. *Journal of Climate*, 16, 281–296.

Morice, C.P., Kennedy, J.J., Rayner, N.A. and Jones, P.D. (2012) Quantifying uncertainties in global and regional temperature change using an ensemble of observational estimates: The HadCRUT4 data set. *Journal of Geophysical Research: Atmospheres*, 117(D8), 1–22.

Neukom, R., Rohrer, M., Calanca, P., Salzmann, N., Huggel, C., Acuña, D., Christie, D.A. and Morales, M.S. (2015) Facing unprecedented drying of the Central Andes? Precipitation variability over the period AD 1000–2100. *Environmental Research Letters*, 10, 084017.

New, M., Hulme, M. and Jones, P. (2000) Representing twentieth-century space-time climate variability. Part II: Development of 1901–96 monthly grids of terrestrial surface climate. *Journal of Climate*, 13, 2217–2238.

Pendergrass, A.G. and Knutti, R. (2018) The uneven nature of daily precipitation and its change. *Geophysical Research Letters*, 45, 11,980–11,988.

Pfahl, S., O'Gorman, P.A. and Fischer, E.M. (2017) Understanding the regional pattern of projected future changes in extreme precipitation. *Nature Climate Change*, 7(6), 423–427.

Polade, S.D., Gershunov, A., Cayan, D.R., Dettinger, M.D. and Pierce, D.W. (2017) Precipitation in a warming world: Assessing projected hydro-climate changes in California and other Mediterranean climate regions. *Scientific Reports*, 7, 1–10.

Quintana, J.M. (2012) Changes in the rainfall regime along the extratropical West coast, 25, 1–22.

Rabatel, A., Francou, B., Soruco, A., Gomez, J., Caceres, B., Ceballos, J.L., Basantes, R., Vuille, M., Sicart, J.E., Huggel, C., Scheel, M., Lejeune, Y., Arnaud, Y., Collet, M., Condom, T., Consoli, G., Favier, V., Jomelli, V., Galarraga, R., Ginot, P., Maisincho, L., Mendoza, J., Ménégoz, M., Ramirez, E., Ribstein, P., Suarez, W., Villacis, M. and Wagnon, P. (2013) Current state of glaciers in the tropical Andes: A multi-century perspective on glacier evolution and climate change. *The Cryosphere*, 7, 81–102.

Ragettli, S., Immerzeel, W.W. and Pellicciotti, F. (2016) Contrasting climate change impact on river flows from high-altitude catchments in the Himalayan and Andes Mountains. *Proceedings of the National Academy of Sciences*, 113, 9222–9227.

Rapaić, M., Brown, R., Markovic, M. and Chaumont, D. (2015) An evaluation of temperature and precipitation surface-based and reanalysis datasets for the Canadian Arctic, 1950–2010. *Atmosphere-Ocean*, 53(3), 283–303.

Rivera, J.A., Marianetti, G. and Hinrichs, S. (2018) Validation of CHIRPS precipitation dataset along the Central Andes of Argentina. *Atmospheric Research*, 213, 437–449.

Sarricolea, P., Herrera-ossandon, M. and Meseguer-Ruiz, O. (2017) Climatic regionalization of continental Chile. *Journal of Maps*, 13, 66–73.

Sarricolea, P. and Romero, H. (2015) Variabilidad y cambios climáticos observados y esperados en el Altiplano del norte de Chile. *Revista de geografia Norte Grande*, 62, 169–183.

Schauwecker, S., Rohrer, M., Acuña, D., Cochachin, A., Dávila, L., Frey, H., Giráldez, C., Gómez, J., Huggel, C., Jacques-Coper, M., Loarte, E., Salzmann, N. and Vuille, M. (2014) Climate trends and glacier retreat in the Cordillera Blanca, Peru, revisited. *Glob Planet Change*, 119, 85–97.

Schauwecker, S., Rohrer, M., Huggel, C., Endries, J., Montoya, N., Neukom, R., Perry, B., Salzmann, N., Schwarb, M. and Suarez, W. (2017) The freezing level in the tropical Andes, Peru: an indicator for present and future glacier extents. *Journal of Geophysical Research*, 122, 5172–5189.

Schneider, U., Becker, A., Finger, P., Meyer-Christoffer, A., Ziese, M., 2018. GPCC full data monthly product version 2018 at 1.0: monthly land-surface precipitation from rain-gauges built on GTS-based and historical data.

Serrano-Notivoli, R., Martín-Vide, J., Saz, M.A., Longares, L.A., Beguería, S., Sarricolea, P., Meseguer-Ruiz, O., Luis de M., 2018. Spatio-temporal variability of daily precipitation concentration in Spain based on a high-resolution gridded data set. *International Journal of Climatology* 38, e518–e530.

Silva, V.B.S., Kousky, V.E. and Higgins, R.W. (2011) Daily precipitation statistics for South America: an intercomparison between NCEP reanalyses and observations. *Journal of Hydrometeorology*, 12, 101–117.

Soares, P.M.M., Cardoso, R.M., Miranda, P.M.A., de Medeiros, J., Belo-Pereira, M. and Espirito-Santo, F. (2012) WRF high resolution dynamical downscaling of ERA-interim for Portugal. *Climate Dynamics*, 39, 2497–2522.

Sun, Q., Miao, C., Duan, Q., Ashouri, H., Sorooshian, S. and Hsu, K.L. (2018) A review of global precipitation data sets: data sources, estimation, and intercomparisons. *Reviews of Geophysics*, 56(1), 79–107.

Uddin, S., Al-Dousari, A., Ramdan, A. and Al Ghadban, A. (2008) Site-specific precipitation estimate from TRMM data using bilinear weighted interpolation technique: an example from

Kuwait. *Journal of Arid Environments*, 72(7), 1320–1328.

Urrutia, R. and Vuille, M. (2009) Climate change projections for the tropical Andes using a regional climate model: temperature and precipitation simulations for the end of the 21st century. *Journal of Geophysical Research – Atmospheres*, 114, 1–15.

Valdés-Pineda, R., Valdes, J.B., Diaz, H.F. and Pizarro-Tapia, R. (2016) Analysis of spatio-temporal changes in annual and seasonal precipitation variability in South America-Chile and related ocean–atmosphere circulation patterns. *International Journal of Climatology*, 36(8), 2979–3001.

Van den Broeke, M.R., Reijmer, C., Van As, D., Van de Wal, R. and Oerlemans, J. (2005) Seasonal cycles of Antarctic surface energy balance from automatic weather stations. *Annals of Glaciology*, 41, 131–139.

Vuille, M., Francou, B., Wagnon, P., Juen, I., Kaser, G., Mark, B. G. and Bradley, R.S. (2008) Climate change and tropical Andean glaciers: past, present and future. *Earth-Science Reviews*, 89, 79–96.

Wilks, D.S. (2006) Statistical Methods in the Atmospheric Sciences. In: *International Geophysics Series*, Vol. 91, 2nd edition. London: Academic Press, p. 627.

Zazulie, N., Rusticucci, M. and Raga, G.B. (2017) Regional climate of the subtropical central Andes using high-resolution CMIP5 models: part I: past performance (1980–2005). *Climate Dynamics*, 49, 1–2.

How to cite this article: Schumacher V, Justino F, Fernández A, *et al.* Comparison between observations and gridded data sets over complex terrain in the Chilean Andes: Precipitation and temperature. *Int J Climatol*. 2020;1–23. https://doi.org/10.1002/joc.6518